

VOXEL SPACE ANALYSIS OF TERRESTRIAL LASER SCANS IN FORESTS FOR WIND FIELD MODELING

A. Bienert^{a,*}, R. Queck^b, A. Schmidt^a, Ch. Bernhofer^b, H.-G. Maas^a

^a Technische Universität Dresden, Institute of Photogrammetry and Remote Sensing, 01062 Dresden, Germany
(anne.bienert, anja.schmidt, hans-gerd.maas)@tu-dresden.de

^b Technische Universität Dresden, Institute of Hydrology and Meteorology, 01737 Tharandt, Germany
(ronald.queck, christian.bernhofner)@tu-dresden.de

Commission V, WG V/3

KEY WORDS: Terrestrial Laser Scanning, Forest, Voxel, Segmentation, Canopy Cover, Eigensystems

ABSTRACT:

Meteorological simulation tools to model gas exchange phenomena within forests require well defined information of forest structure (e.g., 3D forest models) as a basis for the computation of the turbulent flow shaped by the drag of the vegetation. The paper describes techniques to obtain 3D data describing forest stands from dense terrestrial laser scanner point clouds. In a first step, stems are automatically detected from the laser scanner data, forming a basis for the determination of tree density, distance patterns and average stem distance. In a second step, the 3D point cloud is translated into a voxel structure representing the forest. A method to segment voxel clusters with the goal of a tree wise interpretation, is presented. From this voxel structure, drag coefficients can be derived via the local density and distribution of stems, branches and leaves. Therefore different voxel attributes are calculated.

1. INTRODUCTION

The turbulent wind field in forests is dominated by inhomogeneities such as forest clearings and step changes in stand height. Therefore the application of turbulence closure models to describe the momentum absorption by tall canopies depends on (and is limited by) the parameterization of plant architecture (Cescatti & Marcolla, 2004). An improvement of simulation results is anticipated incorporating a more detailed information about 3D vegetation structure. Terrestrial laser scanning is a fast developing new 3D measurement technique which represents an efficient method to capture accurate 3D models of the vegetation. Such a 3D point cloud is a valuable documentation for the spatial biomass distribution. Terrestrial laser scanner point clouds with several million 3D points are not manageable in numerical vegetation models for numeric wind field simulation. Archiving and processing data organisation in a special data structure is needed. Requirements on such a data structure are organisational efficiency and utilisation of memory resources. The administration of huge 3D point clouds is divided in hierarchical and non-hierarchical data structures. Hierarchical structures are based on the recursive subdivision of a region or space. The partition of a 3D space is performed with an octree, i.e. a subdivision of a cube into octants. Non-hierarchical data structures are mostly lists or fixed-grid-methods. The partition into cubes with equal size is advantageous for following implementations. The generalisation of these unorganised point clouds to a discrete 3D raster structure can be realised by filling a fixed-grid-structure, called voxel space.

The central goal of the work presented here is a 3D representation of forest areas, which can be used in numerical wind flow simulation models. The voxel space occupancy gives

information on open areas, and an analysis of the point number and distribution in occupied voxels may be used as a proxy for local wind drag.

3D raster domains derived from terrestrial laser scanner point clouds have also been presented in several other publications in forestry applications. For instance, voxel data are used to identify the structure of laser scanned trees and to reconstruct the stem and branch topology applying skeletonization techniques (Gorte & Pfeifer, 2004; Bucksch & Appel van Wageningen, 2006). Often morphological operators are utilized to reduce noise and fill gaps given by scan shadows (Gorte & Pfeifer, 2004). Aschoff et al. (2006) create a laser scanned voxel space to analyse the flight paths and habitats of bats. Henning & Radtke (2006) use the filled voxel cells to estimate vertical and horizontal plant area index (PAI) profiles. Lefsky & McHale (2008) present a voxel based method to identify stem sections for tree volume estimation. A study from Loudermilk et al. (2007) demonstrates a method to model forest fuel and discusses fire behaviour. Therefore the understorey of a stand was scanned. Due to the resulting voxel space, important information about the fuelbed properties, such as bulk density and vegetation distribution, was derived.

The organisation of the paper is as follows. Section 2 illustrates the study area, data recording and measurement instruments. Methods for determining forest density parameters, the average stem distance and the canopy cover are shown in Section 3. In Section 4, a method is described which transforms laser scanner points into a voxel space. The attributes of each voxel cell and its analysis is the focus of Section 5. Finally, results will be presented (Section 6). An outlook and a summary complete the article.

* Corresponding author.

2. STUDY AREA AND INSTRUMENTS

2.1 Study Area

Since May 2008, intensive measurements at the Anchor Station Tharandter Wald ASTW are conducted. The site is located approximately 25 km southwest of Dresden, Germany (50°57'49"N, 13°34'01"E, 380 m a.s.l.) and is operated by the Institute of Hydrology and Meteorology of the TU Dresden since 1958. A multitude of meteorological, hydrological, ecological measurements and remote sensing observations is available (Bernhofer, 2006). But especially the continuous measurements of momentum, energy and CO₂ flux from the last 15 years and the current investigations of the turbulent exchange processes within and over the spruce stand revealed the need of an advanced vegetation assessment. Most of the common features are described by Feigenwinter et. al (2004) and Grünwald & Bernhofer (2007), so we confine our description to stand features.

The site comprises a forest stand which was established in 1887 and a clearing of 50 m x 90 m, called „Wildacker“. The main canopy is composed of 87 % coniferous evergreen (72 % *Picea abies*, 15 % *Pinus sylvestris*) and 13 % deciduous (10 % *Larix decidua*, 1 % *Betula spec.* and 2 % others) around the clearing. In 2008, the tree density is 335 trees per hectare, the single side leaf area index is 7.1 m²/m² and the mean canopy height around the permanent tower is 30 m. The mean breast height diameter is 33 cm. The ground is mainly covered by young *Fagus sylvatica* (20 %) and *Deschampsia flexuosa* (50 %) (Grünwald & Bernhofer, 2007).

The here presented vegetation assessment is related to wind and temperature measurements made on 4 towers along a transect of the forest clearing (see Fig. 1):

- one permanent scaffolding tower (height 42 m)
- two scaffolding towers (height 40 m) and
- one telescoping tower (height 30 m).

In total 32 measurement points on 4 towers including five at ground level position (2 m), are used to record the turbulent flow with a frequency of 20 Hz. Ultrasonic anemometer (R.M. Young Meteorological Instruments, MI, US) were mounted on booms in a distance of 1 to 3 m to the towers.

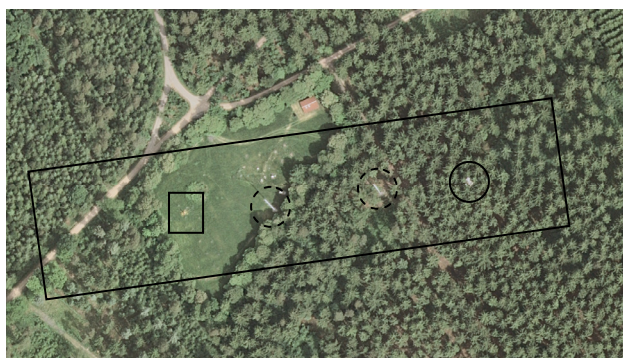


Figure 1. Study area with the clearing „Wildacker“ and the model area (large rectangle); telescoping tower (small square), two scaffolding towers (dashed circles) and one permanent tower (circle)

2.2 Recording

The forest stands around the clearing (500 m x 120 m) were scanned on a windless day with a Riegl LMS-Z 420i and a Faro

LSHE880 terrestrial laser scanner. In total, scans from 13 different ground positions and from the top of the permanent tower (Fig. 2) were taken with an average angular scan resolution of 0.1°. To avoid vibrations on the tower platform during the scanning caused by the operator, the data transfer was managed through WLAN. The scan registration was performed in an automatic manner using a distance pattern of identified tie points. The X axis of the project co-ordinate system was aligned along the spanned line of the towers and the Y axis along North. The origin was defined in the bottom of the permanent tower. The stand is described with approximately 50 million 3D points.

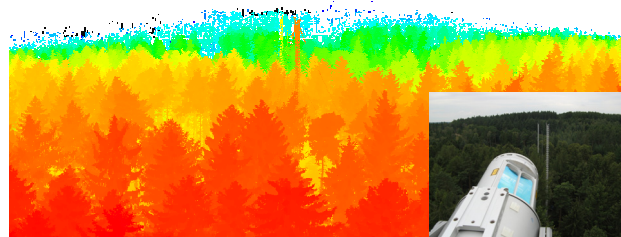


Figure 2. 2D-Intensity Image from the top of the permanent tower along the transect and RGB image with the scanner in position for the ground scanning

3. FOREST DENSITY PARAMETERS

Wind field modelling for complex forests requires additional information regarding the stand density (tree number per area, average tree distance and canopy cover scaled by tree height). Canopy structure also influences light distribution and biodiversity of plants and habitats of animals (Jennings et al., 1999). It also effects the air movements inside a stand.

The forest density parameters were determined in three steps. First an automatic detection of trees in three different horizontal layers of the 3D point cloud was performed. Searching point clusters with a square structure element, potential objects are separated. These objects are classified as trees by fitting a circle. A detailed description of the method is given in Bienert et al., 2007. As a result, we obtained tree number and tree density per hectare. In the second step (Fig. 3) the horizontal distances of a tree to its nearest neighbours were calculated by applying a Delaunay Triangulation. The mean value of all determined distances defines the average tree distance.

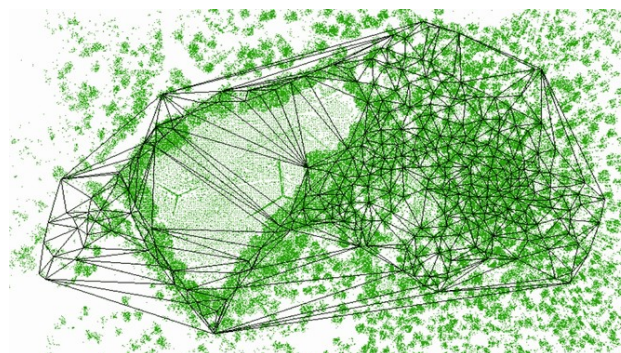


Figure 3. Thinned point cloud with Delaunay Triangulation of automatically detected tree positions

Finally, the Digital Terrain Model (DTM) and the Digital Crown Model (DCM) are established. Both models are produced simultaneously. The heights of the lowest and highest

point inside a 2D raster cell (raster size 50 cm) are stored with the 2D centre point co-ordinates of one cell. Then the normalized Digital Crown Model (nDCM) is calculated by subtracting the DTM height values from the height values of the corresponding DCM cells. The canopy cover is defined as the vertical projection of the canopy per unit area (Jennings et al. 1999). The vertical distribution of the canopy is determined by the probability of pulses in a certain canopy layer.

4. VOXEL DOMAIN

4.1 General

A voxel $V(l,c,p)$ is a cube at a discrete position. A voxel space is built by voxels in a constant horizontal and vertical spacing with the centre point of a voxel cell located at discrete positions l,c,p (line, column, plane) in a Cartesian co-ordinate system. To create a voxel space, the 3D point cloud is transformed into a grid structure. The bounding box ($X_{min}, X_{max}, Y_{min}, Y_{max}, Z_{min}, Z_{max}$) of the point cloud and the voxel size (v_{size}) define the dimension of the voxel space ($l_{max}, c_{max}, p_{max}$). By means of a fixed 3D grid, each point can be allocated to a discrete voxel. In case of free space the cells get the attribute empty or 0. Alternatively, the number of hits N_{Hit} inside the voxel cells is counted. The probability of hits inside the voxel cells is calculated relating the counted hits N_{Hit} to the arriving number of rays at the voxel.

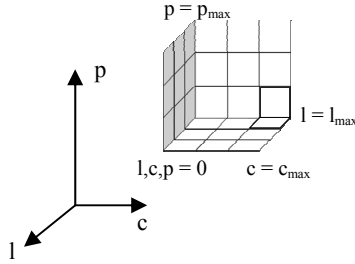


Figure 4. Voxel space with dimension

4.2 Attributes

Per voxel cell different attributes are determined. They can be classified into two different main types of attributes: Statistical values and parameters describing the point distribution. Statistical values are:

- Number of hits N_{Hit}
- Number of penetrations N_{Miss}
- Number of occlusions $N_{Occlusion}$
- Number of included scan positions N_{Scan}
- Reflection probability $P_{Reflection}$

Besides these attributes, further parameters are calculated to describe the point distribution inside each voxel. These parameters include:

- centre point P_0 ,
- principle axes obtained from eigensystems,
- bounding box of the laser scanner points inside a voxel,
- number of clusters with its centre points,
- standard deviation σ_0 .

Analysing these attributes, information about the vegetation density and characteristics per volume (stem wood, branches, twigs or leaves) is derived.

4.3 Ray tracing to determine statistical attributes

A converting of the laser scanner points into the voxel space provides only the number of points inside a voxel cell. Ray tracing represents an efficient method to detect voxels which are penetrated by pulses before they hit an object. The scanner position and the laser scanner point define a ray with a maximum length equal to the maximum range of the range finder of the laser scanner. As a basis for the computation of statistical values, an analysis on the number of laser scanner points inside each voxel N_{Hit} , the number of pulses penetrating the voxel N_{Miss} and the number of pulses before the voxel $N_{Occlusion}$ (occluded rays causing shadows in the inspected voxel) is performed. As scanning is executed from different positions, the number of points inside a cell is counted separately for each position. The hits per cell are determined and summed up using the X_i , Y_i and Z_i co-ordinates of the point i (Eq. 1). So the actual voxel index in l , c and p is calculated.

$$l = \frac{(X_i - X_{min})}{v_{size}} \quad c = \frac{(Y_i - Y_{min})}{v_{size}} \quad p = \frac{(Z_i - Z_{min})}{v_{size}} \quad (1)$$

where v_{size} = voxel size

To find out which ray of a point penetrates a voxel (green voxels in Fig. 5) before hitting an object, the intersection point of the ray R (Eq. 2) with every potential side-face of the cells is calculated. One ray can penetrate two sides of a voxel: The opposing sides or two bordering sides. Using the co-ordinates of the intersection point (intersection of ray with voxel side), the correct cell can be located and counted. The same procedure can be used to track the exit ray of a point (red voxel in Fig. 5). The parameter λ indicates if the intersection point is behind or in front of the actual hit. If λ is smaller than 1, the number of penetration N_{Miss} of the actual voxel increases; if λ is greater than 1 the number of occlusion $N_{Occlusion}$ increases. The voxel including the actual point remains out of consideration. In this case only the number of hits N_{Hit} increases.

$$R: \quad \vec{x} = \vec{p}_1 + \lambda(\vec{p}_i - \vec{p}_1) \quad \lambda \in \mathbb{R} \quad (2)$$

where \vec{p}_1 position vector of scanner position
 \vec{p}_i position vector of scan point i

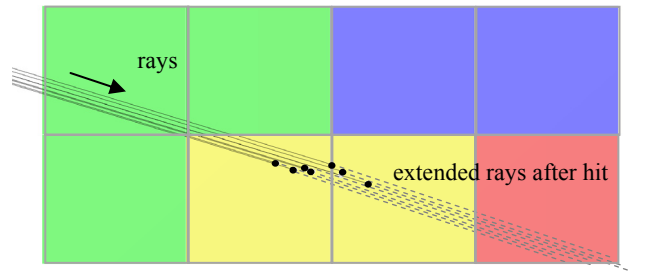


Figure 5. Schematic ray tracing of 7 points in a voxel space (front view); blue = unobserved voxel, yellow = voxel with hits, green = empty voxel with penetration, red = hidden voxel with occlusion from objects before

Counting different attribute numbers (hits, occlusion and miss), the stand is characterised with different types of voxel (Fig. 5 and Tab. 1). These types give information about the stand structure and hidden (completely occluded) areas.

	points	Number of penetrations	occlusions
observed	>0	≥0	≥0
empty	=0	>0	≥0
hidden	=0	=0	>0
unobserved	=0	=0	=0

Table 1. Classification of voxel cells

4.3.1 Reflection probability: The plant area density (PAD) is currently the typical plant parameter implemented in flow models. Using the attributes N_{Hit} , N_{Miss} and $N_{Occlusion}$ a reflection property $P_{Reflection}$ is calculated, which represents PAD. Since some of the flow models use irregular grids the voxel size should not exceed the smallest model resolution. However, the statistical significance limits the reduction of the voxel size. In our case we used 0.5 m. Using simple geometric calculations (superposition of different grids) the derived PAD distribution can be transformed into PAD profiles according to the spatial resolution of the model domain.

Because of different scan positions i , a voxel may include laser measurements from different views. To take these different positions into account, a weighting function w_i is used to determine the reflection probability $P_{Reflection}$ (Eq. 3) with values between 0 and 1. A similar method was presented by Aschoff et al. (2006).

$$P_{Reflection} = \frac{P_i \cdot w_i + P_{i+1} \cdot w_{i+1} + \dots + P_n \cdot w_n}{w_i + w_{i+1} + \dots + w_n} \quad (3)$$

$$\text{with } P_i = \frac{N_{Hit}}{N_{Hit} + N_{Miss}}, \quad w_i = \frac{N_{Hit} + N_{Miss}}{N_{Hit} + N_{Miss} + N_{Occlusion}}$$

where

$P_{Reflection}$ reflection probability of a voxel
 P_i normalised point density of a voxel per scan position
 w_i weighting function of a voxel per scan position
 $i \dots n$ scan position, n = total number of scan positions

5. VOXEL SPACE ANALYSIS

5.1 Voxel space segmentation

The goal of voxel cell segmentation is to separate voxels which belong to different trees. Adjacent voxel are analysed, and connected voxel without gaps define an object. For this purpose, morphological operators known from 2D image processing were adapted on voxel structures. Different types of structure elements can be used. Regarding the nearest neighbours of a voxel, up to 26 adjacent voxels exist (first order). Increasing the order of neighbours e.g. second order with up to 124 adjacent voxel (5x5x5 structure element), gaps between two filled voxels caused by occlusion can be eliminated. Fig. 6 shows different types of first order voxel adjacencies.

A voxel space is built with the dimension of the point cloud and a preset voxel size v_{size} . In a first step, the ground including ground vegetation is extracted by transforming the DTM raster points into the voxel space. Cells containing DTM points and also their 26 neighbour cells belong to the ‘ground’ object. In a second step, a region growing with all remaining filled voxels in a 26-neighbourhood is performed. Voxels with only one

point inside (stray points) are treated as empty. Thus, voxel clusters are built, ideally representing one tree. Normally, more than one cluster present a tree, for instance because of occlusions inside the crown. In a third step smaller clusters are merged in an iterative manner to an adjacent bigger cluster if:

- the 2D distance d between two cluster centre points is smaller than a preset threshold and
- the number n of connected voxels of one segment is smaller as a percentage threshold of the target cluster size n_{target} .

As a result, we obtain a segmented voxel space representing each tree as a different object (number of object), apart from some smaller objects separated by occlusions. By knowing the membership of each voxel to an object, each laser scanner point can be addressed to its object. A biomass determination per tree is achieved by summing up the volumes given by the bounding box of the included points for each filled voxel.

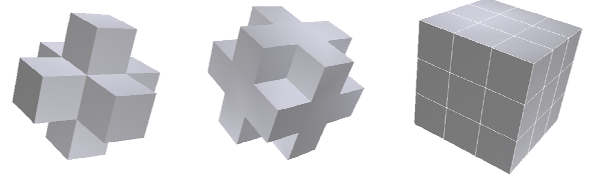


Figure 6. Examples for 3D structure elements with 6-adjacency (left), 18-adjacency (middle) and 26-adjacency (right)

5.2 Eigenvalues and eigenvectors of voxels

The point distribution inside a voxel can be described on the basis of a Principal Component Analysis (PCA) of a point cloud. For a matrix A (Eq. 4) calculated with all points i inside a voxel and its centroid P_0 a symmetric matrix C (Covariance matrix, (Eq. 5)) is calculated.

$$A = \begin{bmatrix} X_i - X_0 & Y_i - Y_0 & Z_i - Z_0 \\ \vdots & \vdots & \vdots \\ X_n - X_0 & Y_n - Y_0 & Z_n - Z_0 \end{bmatrix} \quad (4)$$

$$C = A^T A \quad (5)$$

For this matrix an eigenvector x_k with a corresponding eigenvalue λ_k is given by solving Eq. 6 and further Eq. 7 by using an Identity matrix.

$$C \cdot x_k = \lambda_k x_k, \quad k \in \{0,1,2\} \quad (6)$$

$$(C - \lambda_k I)x_k = 0 \quad (7)$$

where C Covariance matrix
 I Identity matrix
 x_k eigenvector
 λ_k eigenvalues
 X_0, Y_0, Z_0 co-ordinates of the centroid
 X_i, Y_i, Z_i co-ordinates of a point i
 n number of points

After solving Eq. 7, three eigenvalues $0 \leq \lambda_0 < \lambda_1 < \lambda_2$ with corresponding eigenvectors x_k are calculated. Using the eigenvectors, the orientation and direction of the point cloud is given. Furthermore, the eigenvalues represent the variation in each principal direction. In case of a planar point cloud distribution ($\lambda_0 = 0$ and $\lambda_0 \ll \lambda_1, \lambda_2$) the eigenvector x_0 define the

normal vector of the plane. The eigenvectors x_1 and x_2 represents the principal direction of the plane. On the other hand, similar eigenvalues give an indication of an isotropic point distribution. Fig. 7 gives an example of the calculated normalised eigenvectors of sample points inside a 1 m voxel, placed on a tree stem. x_0 defines the normal vector of the stem surface.

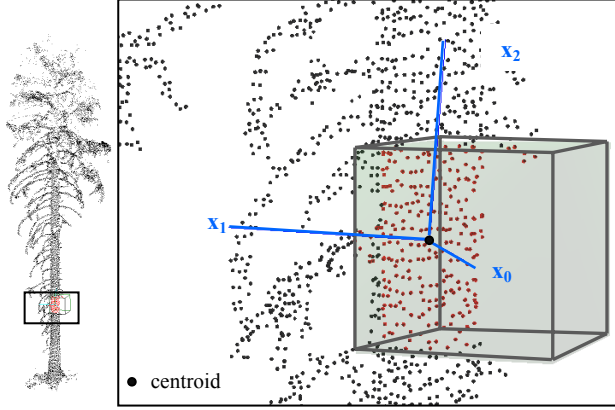


Figure 7. Normalised eigenvectors of sample points (red) of one voxel, x_0 define the normal of the stem surface

6. RESULTS

6.1 Forest Density Parameters

The average tree distance (cmp. Section 3) was determined for the trees around the clearing by applying a Delaunay Triangulation (Fig. 3). A total of 357 trees was detected automatically. The tree distances between the nearest neighbours and their frequencies are shown in Fig. 8. The detected minimum distance d_{min} was 0.54 m and the maximum distance d_{max} was 176.52 m. Finally, the average tree distance d_{mean} was 11.53 m by using all distances. Regarding only distances which pass a simple hypothesis testing (using distances inside 3-sigma border to eliminate large distances located on the border of the model domain), an average tree distance d_{mean} of 9.14 m was received.

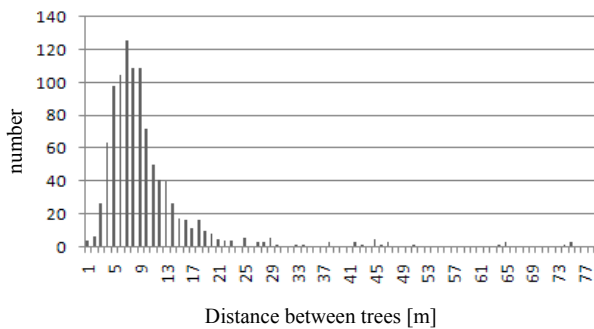


Figure 8. Histogram of detected tree distances by total of 357 trees

Additionally, the stand heights are classified. Fig. 9 shows the model area with height over ground of the canopy top. Six height classes were used (Tab. 2). Due to shadow effects not defined areas occur at the westerly border of the model domain, within these regions no ground or canopy information exists.

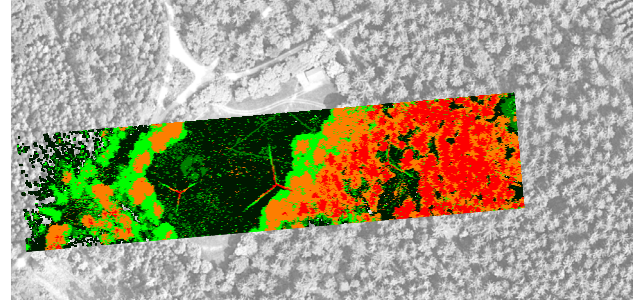


Figure 9. Model area with 5 tree height classes - dark green, green, light green, orange, red

class	vegetation height [m]		%	Area [m ²]
	from	to (\leq)		
dark green	0	1	30.21	4894
green	1	5	8.28	1341
light green	5	15	13.10	2122
orange	15	25	23.55	3815
red	>25		16.26	2634
white (empty)	-	-	8.60	1393

Table 2. Percentage canopy cover of the model area

6.2 Voxel space segmentation

For a 10 m x 10 m area near the permanent tower with 6 spruces, the point cloud was segmented in a 10 cm voxel space, containing 73150 occupied voxels. After a region growing, 3125 segments are separated, including 7 bigger segments for the DTM and six trees. Analysing these segments in a cluster merging step, only 20 segments remain. Fig. 10 shows the point cloud, the region growing before merging with 3125 segments and the final segmentation results with 20 segments left. The ground object contains 20516 voxels and the trees have a segment size between 8592 and 4941 voxels. The remaining segments are built with less than 2382 voxels. Segmented trees give the opportunity to determine local biomass distribution per tree or tree group by summing up all voxels.

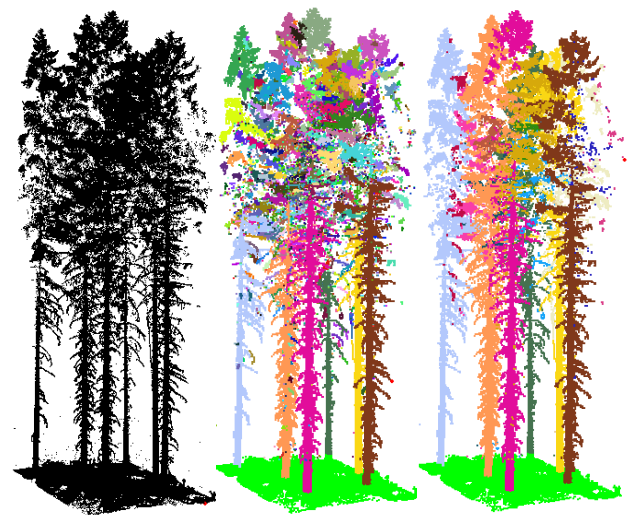


Figure 10. Point cloud of a 10 m x 10 m area (left), segmented voxel space before cluster merging with 3125 segments (middle) and after cluster merging with 20 segments (right)

6.3 Eigenvalues and eigenvectors of voxels

For a test site (10 m x 10 m) inside the stand, a 20 cm voxel space was calculated. Showing only the eigenvector x_2 of the greatest corresponding eigenvalue λ_2 , the principal distribution is described (Fig. 11). The eigenvector was placed in the centroid P_0 with a length equal to its bounding box inside the voxel. As one can see in Fig. 11, the eigenvectors give a good approximation for the branch structure. When using a small voxel size, the eigenvector x_2 depicts the stem surface. Using bigger voxel sizes (e.g. 1 m), the eigenvector x_2 presents the direction of the stem, because the points are distributed in height.

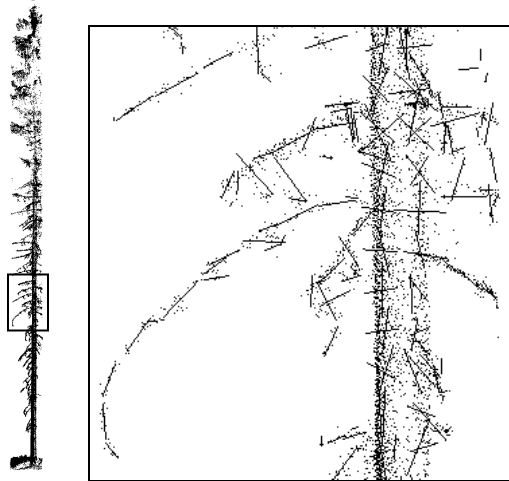


Figure 11. Point cloud of a spruce (left); detailed view of a point cloud with obtained eigenvector from the greatest eigenvalue inside a 20 cm voxel space

7. SUMMARY AND OUTLOOK

The paper presents methods to analyse forest stands concerning stand height, tree density and plant area density (PAD). A proxy for the PAD is derived by generating a 3D voxel space from laser measurements using several views. Furthermore the voxel domain was used to separate voxels which belong to one vegetation object and to analyse local point distribution applying eigensystems. The presented method to separate trees in voxel space gives good results for conifer stands, with non-overlapping tree crowns. Broadleaf stands with dominating trees and overlapping trees are more difficult to handle. The voxel size has to be smaller than the smallest gap between two trees, to separate successfully.

Within this work the point distribution within the voxel was determined (eigenvector, standard deviation, bounding box, centre point). We aim to automatically classify the vegetation elements inside a voxel in a next step. A feasible approach could use the specific voxel attributes to indicate vegetation elements. Stems have a different influence on turbulence formation than branches or twigs with needles. Knowledge of position and type of the vegetation elements could be implemented in the derivation of flow model parameters.

ACKNOWLEDGEMENT

The research work presented in this paper is funded by the German Research Foundation (DFG) in the SPP 1276 "Metström" in the collaborative project "Turbulent Exchange processes between Forested areas and the Atmosphere" at the

Technische Universität (TU) Dresden. The authors would thank FARO Europe for providing the laser scanner and the software *FARO Scene*.

REFERENCES

- Aschoff, T., Holderied, M.W., Spiecker, H., 2006. *Terrestrische Laserscanner zur Untersuchung von Wäldern als Jagdlebensräume für Fledermäuse*. In: Photogrammetrie - Laserscanning - Optische 3D-Messtechnik (Beiträge Oldenburger 3D-Tage 2006, Hrsg. Th. Luhmann und C. Müller), Verlag Herbert Eichmann, pp. 280-287.
- Bernhofer, Ch. (Hrsg.), 2002. *Exkursions- und Praktikumsführer Tharandter Wald*. Material zum "Hydrologisch-meteorologischen Feldpraktikum". Tharandter Klimaprotokolle (ISSN 1436-5235), Band 6, 292 pp.
- Bienert, A., Scheller, S., Keane, E., Mohan, F., Nugent, C., 2007. *Tree detection and diameter estimations by analysis of forest terrestrial laserscanner point clouds*. International Archives of Photogrammetry, Remote Sensing and Spatial Information Sciences, Vol. XXXVI, Part 3/ W52
- Buksch, A. & Appel van Wageningen, H., 2006. *Skeletonization and segmentation of point clouds using octrees and graph theory*. International Archives of Photogrammetry, Remote Sensing and Spatial Information Sciences, Vol. XXXVI, Part 5
- Cescatti, A. & Marcolla, B., 2004. *Drag coefficient and turbulence intensity in conifer canopies*. Agricultural and Forest Meteorology, 121(3-4), pp. 197-206.
- Feigenwinter, C., Bernhofer, C., Vogt, R., 2004. *The influence of advection on the short term CO₂-budget in and above a forest canopy*. Boundary-Layer Meteorology 113, pp. 219-224.
- Gorte, B., 2006. *Skeletonization of Laser-Scanned Trees in the 3D Raster Domain*. Innovations in 3D Geo Information Systems, Springer Berlin Heidelberg, pp. 371 – 380.
- Gorte, B. & Pfeifer, N., 2004. *Structuring laser-scanned trees using 3D mathematical morphology*. International Archives of Photogrammetry, Remote Sensing and Spatial Information Sciences. Vol. 35, Part B5, pp. 929-933.
- Grünwald, T. & Bernhofer, Ch., 2007. *A decade of carbon, water and energy flux measurements of an old spruce forest at the Anchor Station Tharandt*. Tellus 59B, pp. 387–396.
- Henning, J.G. & Radtke, P.J., 2006. *Ground-based laser imaging for assessing three-dimensional forest canopy structure*. Photogrammetric Engineering and Remote Sensing, Vol. 72 (12), 2006, pp. 1349-1358.
- Jennings, S.B., Brown, N.D., Sheil, D., 1999. *Assessing forest canopies and understory illumination: canopy closure, canopy cover and other measures*. Forestry 72(1), pp. 59–74.
- Lefsky, M. & McHale, M.R., 2008. *Volume estimates of trees with complex architecture from terrestrial laser scanning*. Journal of Applied Remote Sensing 2(1).
- Loudermilk, E.L., Singhania, A., Fernandez, J.C., Hiers, J.K., O'Brien, J.J., Cropper Jr., W.P., Slatton, K.C., Mitchell, R.J., 2007. *Application of ground-based lidar for fine-scale forest fuel modelling*. In: Butler, Bret W.; Cook, Wayne, comps. 2007. The fire environment-innovations, management, and policy; conference proceedings. Destin, FL. Proceedings RMRS-P-46 CD. pp. 515 – 523.